International Journal of Impact Engineering 180 (2023) 104662

Contents lists available at ScienceDirect

International Journal of Impact Engineering

journal homepage: www.elsevier.com/locate/ijimpeng

A novel numerical method for stochastic study of fiber-reinforced composites with nanoparticles under impact loading

Dayou Ma [a,*], Christian Matheus dos Santos Cougo [b], Sandro Campos Amico [b], Marco Giglio [a], Andrea Manes [a]

[a] Politecnico di Milano, Department of Mechanical Engineering, via la Masa, 1, Milan 20156, Italy
[b] Federal University of Rio Grande do Sul, Av. Bento Gonçalves, 9500. Porto Alegre, 91501-970, Brazil

ARTICLE INFO

Keywords:
Low velocity impact
Finite element method
Distribution of nanoparticles
Inhomogeneity
Fiber-reinforced composites

ABSTRACT

Nanoparticle-reinforced composites have caught attention due to their enhanced properties and wide potential use. However, the uncertainty in the distribution of nanoparticles during the manufacturing poses several challenges when deterministic numerical methods are used to model their mechanical behavior, following a macro homogeneous approach. In this work, a stochastic numerical method based on finite element modeling is proposed to simulate the inhomogeneous distribution of nanoparticles inside the composite, focusing on low-velocity impact. Each element in the finite element model is regarded as a unit cell with a constant weight fraction of nanoparticles, while the random distribution of nanoparticles is described by a variable weight fraction among elements following a Gaussian distribution. This distribution is related to the mechanical behavior of the unit cell inside the model and it was defined based on material characterization tests for different nanoparticles weight fractions. To validate the proposed model, experimental low-velocity impact tests, at different energy levels, on composites reinforced with nanoparticles (0.5 wt.%) were carried out. The numerical method was assessed by comparing experimental results in terms of mechanical response and damage phenomena. The current numerical methodology was found to contribute to uncertainty investigation based on a mixed experimental-numerical analysis.

1. Introduction

Fiber-reinforced polymers filled with nanoparticles have been attracted great attention due to their enhanced properties and a varied potential use, such as in structural health monitoring via electrical conductivity. However, the random and inhomogeneous distribution of nanoparticles inside the composite poses a challenge for optimal design based on predictive numerical modeling especially when a macro-homogenous approach is considered.

Finite Element (FE) modeling of such materials tackles several issues, including large variability in mechanical properties, time-consuming calculation and complex model generation, as widely mentioned in the literature [1–3]. Indeed, the presence of nanoparticles increases complexity of a damage model conceived involving multiscale evaluation, especially for structural analysis, and a massive computational cost may arise for complex loading conditions (*e.g.*, impact cases). Thus, investigation of reliable and efficient modeling strategies for assessing the effect of an inhomogeneous distribution of nanoparticles that allow application into a larger modeling scale with reasonable accuracy is a key aspect to advance the understanding of damage behavior of nanocomposites for a wider application.

The inhomogeneous distribution of nanoparticles inside composites have been investigated in many experimental works. Transmission electron microscopy has been used to show that nanoparticles do not spread uniformly during manufacturing, but their distribution follows a Gaussian distribution [4]. This may lead to defects inside composites, such as agglomeration and voids, resulting in unpredictable mechanical behavior [5–7]. Larger scatter in both strength and modulus of nanoparticle-reinforced polymers was noticed for higher weight fractions [8], a reflection of the effect of inhomogeneous distribution of nanoparticles [9]. Besides, the distribution of nanoparticles has a significant effect on the failure phenomena, as concluded from the observation of inner defects [5,10]. Most of the cited research used coupon-level samples under simple loading conditions, which allows

* Corresponding author.
E-mail address: dayou.ma@polimi.it (D. Ma).

https://doi.org/10.1016/j.ijimpeng.2023.104662
Received 31 December 2022; Received in revised form 27 February 2023; Accepted 21 May 2023
Available online 29 May 2023

observation of nanoparticles distribution inside the samples before and after testing [11]. However, analysis of their effect for more complex loading conditions, like impact cases, is limited.

Numerical modeling of nanocomposites taking into account uncertainty has been reported [12–14]. Their uniaxial mechanical behavior can be simulated by representative volume elements using finite element methods [9,15,16], while molecular dynamics methods can be applied for an accurate prediction by detailing the structure of nanocomposites, although demanding long calculation times [17,6]. Besides, with refined finite element modeling on a large scale, the effect of reinforcement waviness and agglomeration of nanoparticles on mechanical parameters can be analyzed, although time and calculation costs are high [18]. Compared with these numerical methods, multiscale modeling approaches may be preferable for the modeling of large structures, or even at components and subcomponents level under complex loading conditions [19–21], where mechanical parameters obtained from smaller-scale modeling can be used for simulations at a larger scale [22,23]. This approach is regarded as an effective way to fill the size gap between microfibers and nanoparticles.

Advanced numerical methods allow the modeling of nanoparticles inside composites at coupon scale, like the application of the modified peridynamic method for capturing their fracture behavior [24], while the random field can be introduced into typical finite element method to generate randomness in the composite. These methods are feasible to account for nanoparticles distribution [25], but uncertainty investigations mostly focused on a limited scale due to the complexity of the numerical algorithm and the massive calculational cost for modeling uncertainty features. Even at nano-scale and/or micro-scale, the use of this method is not straightforward, leading to rare applications for complex loading conditions as impacts. Besides, for an uncertainty study by modeling, specific material parameters need to be calibrated from experiments for quantitative validation [7,26]. But considering the homogeneous method applied in such methods, it is difficult to introduce the effect of nanoparticles distribution. Besides, the experimental effort may not cover all possible mechanical/damage phenomena, and the quantification of uncertainty is not straightforward considering the non-uniform distribution of nanoparticles. All this emphasizes the difficulties in correlating numerical modeling and experimental tests for uncertainty studies in nanocomposites.

In this work, a novel method based on finite element modeling is proposed to characterize the inhomogeneous distribution of nanoparticles using a macroscale modeling approach but with a statistically discrete distribution of mechanical properties. The method was applied to an aramid/epoxy composite with 0.5 wt.% nanoparticles tested under low-velocity impact at two different energies to analyze its effect on damage morphology of the composite with either uniform or non-uniform distributions of nanoparticles. Material properties, calibrated from tensile, compressive and shear tests were determined on aramid-epoxy composites with 0, 0.5, 1.0 or 2.0 wt.% of nanoparticles and assigned to each element to create a random distribution of nanoparticles based on statistical analysis to capture the inhomogeneity effect on the mechanical response.

2. Experimental activities

2.1. Material preparation

The nanofillers used in the present study were multi-walled carbon nanotubes (CNTs) from Chengdu Organic Chemicals Co. (diameter range: 10–30 nm, length: ≈30 μm and 85% purity), and graphene nanoplatelets (GNPs) from Strem Chemicals Co. (thickness: 6–8 nm, width: 25 μm). Kevlar™ 29 plain-weave fabric from DuPont was used (density: 1440 kg/m^3, thickness: 0.50 mm). A DGEBA resin named Ampreg 26, with a high glass-transition temperature hardener, from Barracuda Composites was used.

Regarding the manufacturing process, the two nanoparticles (weight ratio of 1:1) were dispersed in a solution of 60% acetone and 40% ethanol using an ultrasonic sonicator mixer VibraCell VCX750 (frequency: 20 kHz) with an amplitude of 250 W for 45 min, repeatedly vibrating for 25 s followed by a 10 s pause. The resulting mixture was evenly spread over both sides of a dried fabric to obtain a random distribution of nanofillers. Four different weight fractions of nanoparticles were studied, *i.e.,* 0, 0.5, 1.0 and 2.0 wt.%. Eight layers of nanoparticle-impregnated fabrics were positioned and sealed for the vacuum infusion process. The epoxy was later cured for 24 h at room temperature and post-cured for 6 h at 80 °C, as recommended by the resin manufacturer. A schematic of the process can be found in Fig. 1. Specimens were cut from the cured laminate using a Waterjet Cutter machine.

2.2. Material characterization

In order to obtain the material properties of the composites, material tests including tensile, compressive and shear were carried out on the samples with 0, 0.5, 1.0 and 2.0 wt.% hybrid nanofillers. All tests were performed on thin samples (thickness: 2.5 mm). Tensile tests were carried out on (250 × 25) mm specimens according to ASTM D3039 at a loading rate of 2 mm/min with extensometers monitoring strain in orthogonal directions. Compressive tests were conducted according to ASTM D6641 on (13 × 2.5) mm specimens at a loading rate of 1.3 mm/min. And V-notched rail shear tests were carried out at 2 mm/min following ASTM D7078 to obtain in-plane shear properties. Five samples were tested in each case. Moreover, short-beam tests according to ASTM D2344 were carried out for the composite with 0.5 wt.% nanoparticles to assess the interfacial property useful to the impact simulation. Detailed experimental data can be found in [26]. The average values of experimental results in each group, as listed in Table 1, were used in the numerical model.

2.3. Low-velocity impact tests

Low-velocity impact (LVI) tests were conducted according to ASTM D7136. The impact load was recorded with a Quartz Force Link Type 9331B load-cell, and the impact velocity was collected with a two-flag-prong photoelectric sensor model E3FALP21 from OMRON. The mass of the impactor was 2.303 kg and two energy levels were used, 15 J and 30 J. The samples were completely fixed on a rigid frame to prevent movement during impact. The obtained experimental data was filtered based also on ASTM D7136, as described in [27]. More details of the LVI tests with respect to failure phenomena and load-displacement curves can be found in [26].

3. Numerical method

3.1. Overview

An experiment-based stochastic numerical method considering the random distribution of nanoparticles inside the composites was proposed to investigate their effect on the mechanical response under impact loading. An overview of the method can be found in Fig. 2. Starting from the material tests, the basic mechanical properties (tensile, compressive and shear) of the nanocomposites were obtained, helping the determination of material models considering different weight fractions. The samples used for that are smaller than those for the impact tests and, in the former, the nanoparticles were assumed to be uniformly distributed, focusing on the effect of nanoparticle distribution on the impact structural level.

To efficiently describe the distribution of nanofillers, each element in the model was regarded as a unit cell, with a varying weight fraction (and therefore mechanical properties) from element to element, but the content of nanoparticles is considered constant within the volume of each element during the simulation. Therefore, the distribution of nanoparticles can be described based on different material models with

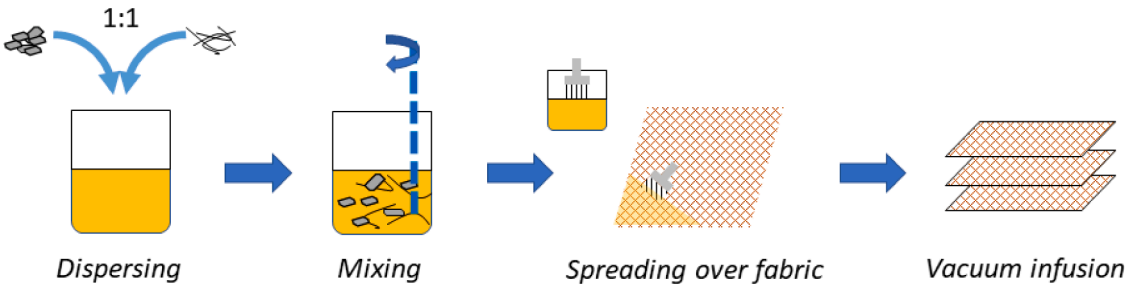

Fig. 1. Manufacture process of nanoparticle-reinforced composites.

Table 1
Mechanical properties for the composites with different weight fractions of nanoparticles.

Mechanical properties		0.0		0.5%		1.0%		2.0%		Note
		0°	90°	0°	90°	0°	90°	0°	90°	
Tensile	Modulus (GPa)	15.2	19.6	16.8	19.7	20.1	19.2	17.0	17.3	
	Strength (MPa)	380.6	496.7	384.3	497.9	513.7	486.8	411.0	396.9	Applied as X_t=Y_t in Eqs. (1,2)
Compressive	Strength (MPa)	94.4	112.6	97.2	108.3	106.1	116.3	102.9	110.4	Applied as X_c=Y_c in Eqs. (3,4)
In-plane shear	Modulus (GPa)	1.56		1.65		1.65		1.50		
	Strength (MPa)	30.2		38.0		32.5		32.4		Applied as S_c in Eqs. (1, 2, 5)

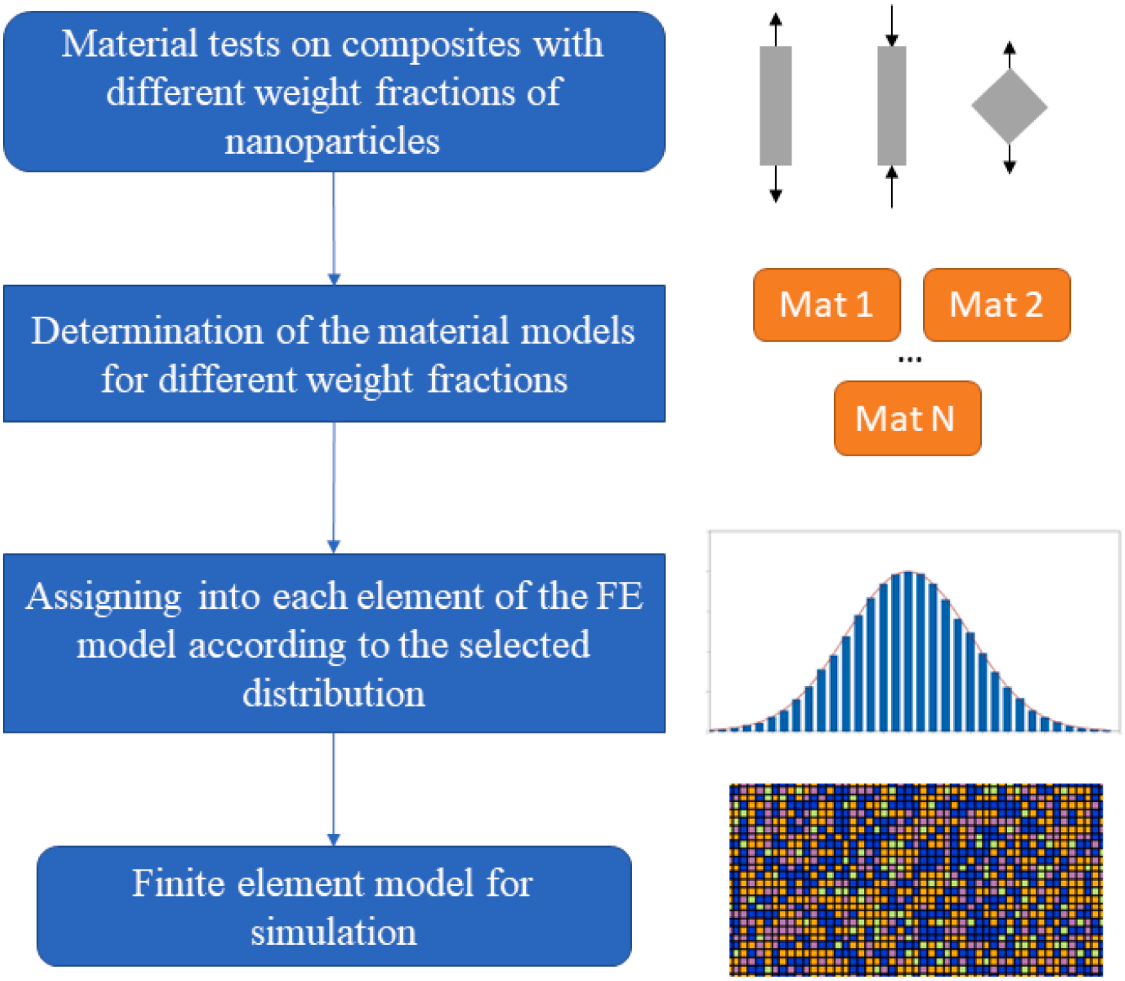

Fig. 2. Overview of the stochastic numerical method.

varying weight fractions being assigned to each element, where different mechanical parameters for both elastic behavior and damage process were applied according to the weight fractions. Besides, the Monte-Carlo method was applied to randomly generate and run the calculation for different models for a comprehensive understanding of the effect of the stochastic distribution of nanoparticles.

3.2. Material damage model

Each layer of the composite was modeled as an orthotropic material using the MAT_ENHANCED_COMPOSITE_DAMAGE (MAT_054/055) material damage model, which is based on the Chang-Chang [28] failure criteria (MAT_054). This damage model has been successfully applied in the simulation of impact events [29]. For the fiber damage, in-plane failure criterion under tension was applied, shown in Eqs. (1) and (2), while the compressive failure criteria is described in Eqs. (3) and (4). The failure criterion for the matrix is shown in Eq. (5) [32].

$$e_{ft_x}^2 = \left(\frac{\sigma_{11}}{X_t}\right)^2 + \beta\left(\frac{\sigma_{12}}{S_c}\right)^2 - 1 \begin{cases} \geq 0, failed \\ 0, elastic \end{cases} \tag{1}$$

$$e_{ft_y}^2 = \left(\frac{\sigma_{22}}{Y_t}\right)^2 + \beta\left(\frac{\sigma_{12}}{S_c}\right)^2 - 1 \begin{cases} \geq 0, failed \\ 0, elastic \end{cases} \tag{2}$$

$$e_{fc_x}^2 = \left(\frac{\sigma_{11}}{X_c}\right)^2 - 1 \begin{cases} \geq 0, failed \\ 0, elastic \end{cases} \tag{3}$$

$$e_{fc_y}^2 = \left(\frac{\sigma_{11}}{Y_c}\right)^2 - 1 \begin{cases} \geq 0, failed \\ 0, elastic \end{cases} \tag{4}$$

$$e_m^2 = \left(\frac{\sigma_{12}}{S_c}\right)^2 - 1 \begin{cases} \geq 0, failed \\ 0, elastic \end{cases} \tag{5}$$

where X_t and Y_t are the in-plane tensile strengths of the composite, X_c and Y_c are the compressive strengths, and S_c is the in-plane shear strength. The parameter β is used to describe shear behavior during loading, and β=0 is recommended for a more precise comparison with the experiments [32]. After the failure criterion is met, damage appears in the related elements, and the strength drops to a specific value until the element is deleted by meeting the strain threshold in MAT_054.

The properties obtained with the material characterization tests for the material models are compiled in Table 1, with 0 to 2.0 wt.% nanoparticle weight fraction. Considering the variation in experimental data, the average values were used, which have been calibrated numerically and employed in the related simulations [26].

As for interlaminar damage, the tiebreak contact was applied among layers of the composite to allow modelling of delamination through the failure of contact when the strength of the interface is reached [30]. That strength was set as 62.8 MPa in the normal direction and 28.3 MPa in shear, based on short beam test results.

3.3. Stochastic modeling

Based on experimental observations, the distribution of nanoparticles inside the composite has been reported to obey a Gaussian distribution [4], whose probability density function is shown as Eq. (6),

$$f(x) = \frac{1}{\sigma\sqrt{2\pi}} e^{\frac{-1}{2}\left(\frac{x-\mu}{\sigma}\right)^2} \tag{6}$$

where σ is the standard deviation and μ is the mean value for the distribution.

Based on that, a stochastic model for nanoparticles was built in the finite element model where each element has a constant weight fraction. The weight fraction of nanoparticles varies from 0.0 to 2.0 wt.% (see Fig. 3a) in the elements following the Gaussian distribution presented in Fig. 3a. The parameter μ in Eq. (6) can be determined by the designed weight fraction of the impact target, which was set to 0.5 wt.%. The standard deviation can be determined according to the range of weight fractions in the tested materials.

Following this methodology, the local inhomogeneous distribution can be replicated while the global weight fraction is guaranteed. And since all material parameters for composites with different nanoparticles content were obtained from tests, like the current case according to Table 1, reliability of the simulation increases. Besides, the variation in spatial distribution was considered in this work to cover more possibilities in the stochastic model for the investigation of the nanoparticles effect, which varies from *Cases 1–6* in the model for the same weight fraction. Furthermore, a uniform model with uniform material parameters for the 0.5 wt.% nanofillers was built as a reference, which is named as *Case 0*. For the calculation of the proposed method, it takes 50 min for each case to run with 15 CPUs (E5–2630 2.40 GHz 15 cores/30 threads – 128 GB RAM).

3.4. Numerical setup

In the numerical model, a rigid body was used for the impactor considering no deformation during impact. The initial velocity of the impactor was assigned to replicate the impact loading with an energy of 15 and 30 J. Regarding boundary conditions, the red region in Fig. 3b was fully fixed to simulate the frame fixture in the impact. Besides, the automatic surface-to-surface contact behavior was used for simulating the contact between impactor and target. Definition of the mesh size is critical for the simulation with the finite element method, especially for stochastic modeling. Therefore, a mesh sensitivity study was performed prior to modeling the composites with nanoparticles based on the experimental data for impact tests at 15 J. The 1.0-mm-side-mesh was

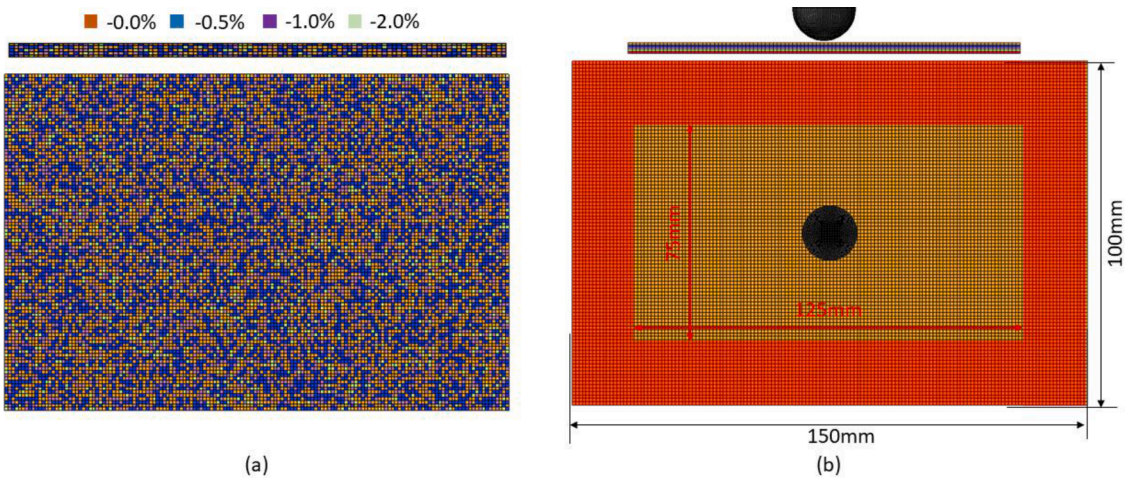

Fig. 3. Stochastic modeling with finite element method.

selected for the current work, allowing reliable results with acceptable calculation time.

4. Results and discussions

The comparison of experimental and numerical results with respect to both load history and force-displacement curves at 15 J impact energy can be found in Fig. 4. The spatial distribution influences the impact results, *i.e.*, contact time, residual displacement and peak load, especially the latter, for which a significant variation was obtained for the different cases (about 20%). On the other hand, only a small difference in slope of loading was observed among the cases.

Regarding the comparison between stochastic (*Cases 1–6*) and uniform (*Case 0*) models, average simulation curves (see the dark line) are used in Fig. 4. The peak load is higher for the uniform model than for the average one from the stochastic model, although *Case 1* and *Case 3* also reached such high loads. Furthermore, some features of the curves were captured by the stochastic model. A significant drop in load after the peak found in the experimental data is not seen on either average or uniform curves, but it is noticed in *Case 4*. As shows Fig. 5, where the distribution of nanoparticles near the impact center has been magnified, some elements without nanoparticles (0 wt.%, blue-colored) are grouped (highlighted in the figure) near the impact point in *Case 4*, which reduces local material properties, compared with other regions with a denser distribution of nanoparticles, and may lead to premature local failure. Indeed, a sudden drop in loading can be identified in Fig. 4, indicating that the distribution of nanoparticles can influence the mechanical performance of the nanocomposites, especially near the impact center. Overall, the change in mechanical response due to the difference in distribution, especially at/near the impact point, is significant, which indicates the capability of stochastic modeling to address nanocomposites uncertainty issues.

The indentation that occurred after impact is shown in Fig. 6. That region was divided into four parts in relation to the impact center, as displayed in Fig. 6a, to assess damage. Besides, indentation in the damage zone was also measured to estimate the damage volume, which is considered as a cone (see Fig. 6b). This allows to quantitatively assess the deformation near the impact region and to compare experimental and numerical results.

Damage characterization for an impact energy of 15 J is reported in Table 2. From the experimental results, the damage/deformation of the target indeed shows a deviation from the impact center. Such a deviation cannot be replicated by a uniform model, but stochastic models can capture this phenomenon in different cases. The obtained range of experimental deviations was 0 - 3.2 mm, which covers the difference in damage length from the impact center, *i.e.*, the difference between *a* and *b*, and/or *c* and *d* in Fig. 6a.

The correlation between absorbed energy and damage volume can be found in Fig. 7. For a small variation in absorbed energy, the damage volume can significantly vary, as highlighted in Fig. 7 (see *Case 5*), which ratifies the effect of the nanoparticle distribution.

At higher impact energy (30 J), penetration occurred in the tests, as indicated in Fig. 8. The loading history with respect to both slope and peak load is similar for all stochastic models, which show a significant reduction in peak load compared to the uniform model. In addition, the experimental data are located between the uniform and the stochastic models.

Regarding damage characterization for the impact at 30 J, for which penetration occurred, the damage dimension along the longitudinal direction was measured based on the total crack length along the transverse direction. The deviations of all model cases in relation to the experiment is compiled in Table 3, which shows a reduction in percentage deviations compared to those found for 15 J. For *Case 0* and *Case 6*, the damage along the length direction is less affected by the distribution of nanoparticles, while the range of deformation from the stochastic models can still cover the experimental results. However, based on both loading history and deviations of the damage region, the effect of nanoparticles distribution is less significant when the energy increases from 15 to 30 J.

Based on the proposed numerical method, the effect of the nanoparticles on strength is less significant than that on modulus (as listed in Table 1). As the impact energy is low, the number of failed elements is limited and most elements retain an elastic behavior, indicating the importance of the elastic modulus in describing the mechanical behavior. However, as energy increases, more elements fail, therefore, strength grows in importance and the relevance of the fabric architecture and fiber content increases. However, the effect of the nanoparticles distribution is mainly on the matrix and the interface between fiber and matrix, and this effect is reduced as the energy increases.

Fig. 9 shows the correlation between absorbed energy and damage volume for the 30 J impact. The height of the damage cone was obtained from the tests, *i.e.*, the maximum displacement of the impactor when penetration occurred. In this figure, different damage volume values can be noticed for similar absorbed energy levels, as previously observed for the 15 J impact.

The penetration history with respect to different layers was also investigated, as shown in Fig. 10. The contact period between target and impactor before the peak was divided into three regions together with the peak load point, as presented in Fig. 10 (right). Region A represents the elastic response of the target, region B starts in the first drop in load, and region C contains the further reduction of the contact load before reaching the peak. The gray color in Fig. 10 represents the non-cracked region.

According to Fig. 10, the stochastic models can provide a longer

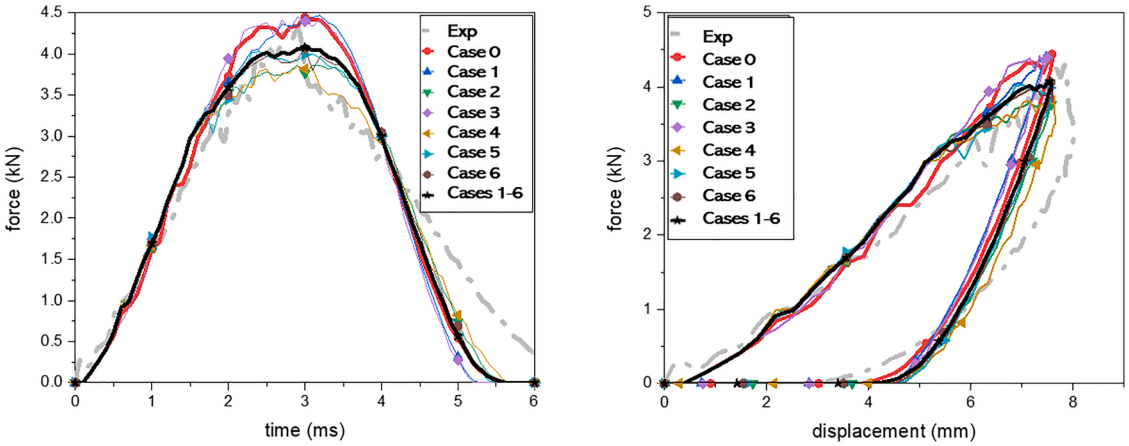

Fig. 4. Mechanical response of the composite for 15 J impact energy; the dark line (*Cases 1–6*) represents the average curve of simulations.

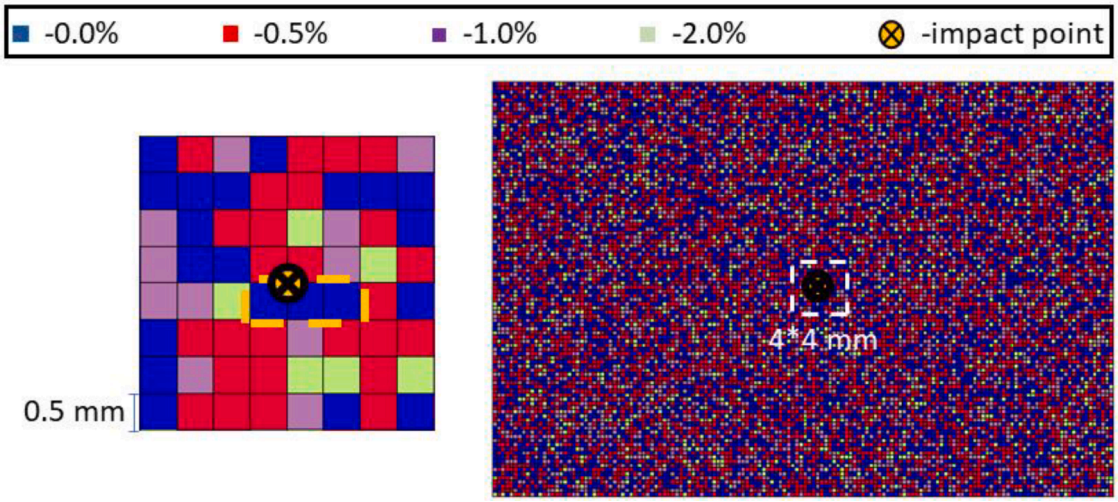

Fig. 5. Distribution of nanofillers in the numerical model near the impact region (*Case 4*).

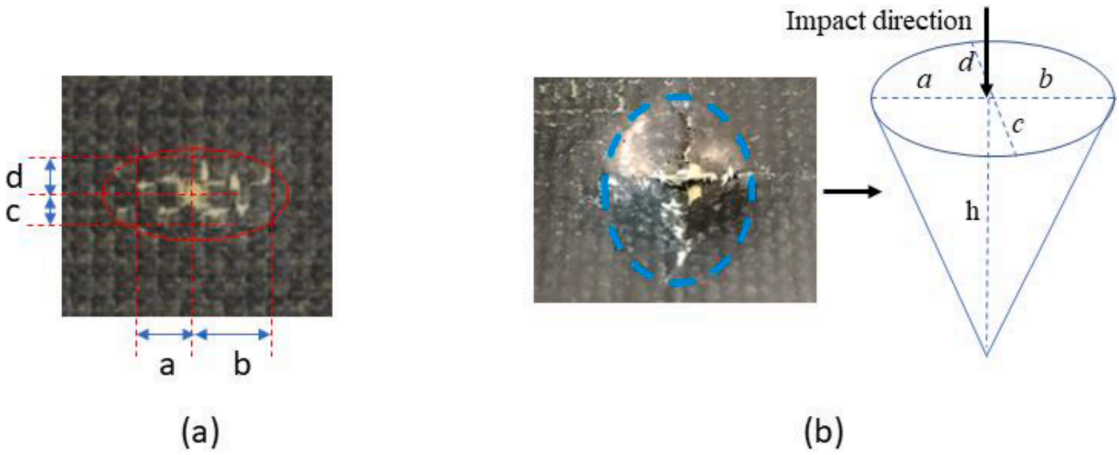

Fig. 6. Damage characterization after the low-velocity impact.

Table 2
Damage characterization from numerical and experimental results for an impact energy of 15 J.

Length (mm)	Experiment	*Case 0*	*Case 1*	*Case 2*	*Case 3*	*Case 4*	*Case 5*	*Case 6*	*Cases 1–6*
a	4.0	4.0	3.3	7.0	4.4	7.3	6.1	6.3	5.7
b	5.5	4.1	6.4	7.4	5.4	7.4	7.6	7.5	7.0
c	2.0	1.0	0.5	0.2	1.2	0.0	0.1	0.0	0.3
d	2.6	1.0	2.8	3.4	1.7	2.8	3.3	2.7	2.8
Longitudinal deviation	1.5	0.1	3.1	0.4	1.0	0.1	1.5	1.2	1.3
	(16%)	(1%)	(32%)	(3%)	(10%)	(1%)	(11%)	(9%)	(10%)
Transverse deviation	0.6	0	2.3	3.2	0.5	2.8	3.2	2.7	2.5
	(13%)	(0)	(70%)	(89%)	(17%)	(96%)	(94%)	(100%)	(81%)

propagation history, from the failure of the first layer to the last one, as shown by the different colors, *i.e.,* an earlier initiation of the crack on the back-side layer starting from region A for most cases in the stochastic model compared to the uniform model, which begins in region C. The accelerated crack initiation is due to the non-uniform distribution of nanoparticles, causing stress concentrations coupled with low local strength, while failure of the composite can be slowed down with varying material properties along the loading direction, *i.e.,* the crack tip along the thickness direction covering multiple layers, leading to a long propagation history. Besides, layer cracking can cause changes to the loading curves, while full penetration occurs at the onset of the peak load for all cases.

5. Conclusions

In the current work, a stochastic model was proposed to describe the inhomogeneous distribution of nanoparticles in composites, being considered an efficient methodology for uncertainty investigations. In the finite element model, each element is regarded as one unit cell with a constant weight fraction of nanoparticles. Weight fractions are related to the mechanical behavior of the unit cell inside the model. As a result, the model can simulate the inhomogeneous distribution with different filler contents at different regions of the impacted panel. A Gaussian distribution was used to describe the distribution of nanoparticles, and a uniform material model was used as reference. The stochastic model

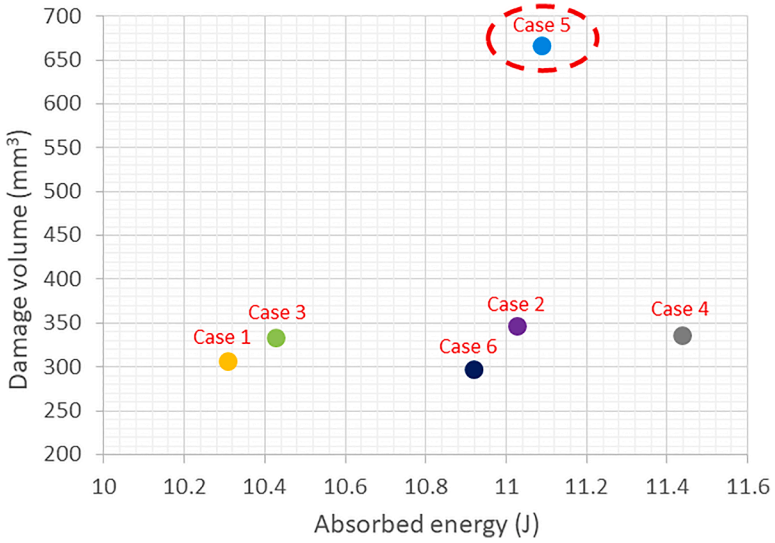

Fig. 7. Correlation between absorbed energy and damage volume for an impact energy of 15 J.

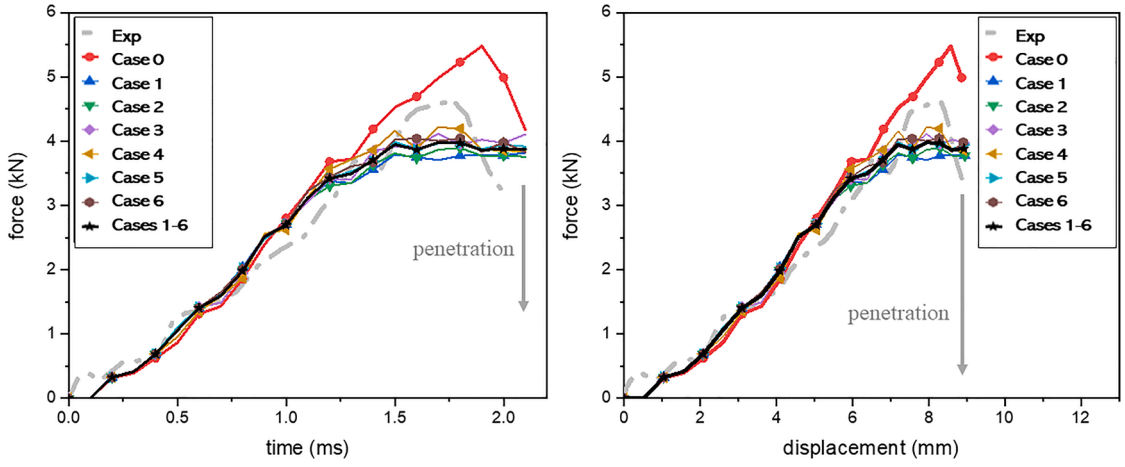

Fig. 8. Mechanical response of the composite for an impact energy of 30 J.

Table 3
Damage characterization from numerical and experimental results for an impact energy of 30 J.

Length (mm)	Experiment	*Case 0*	*Case 1*	*Case 2*	*Case 3*	*Case 4*	*Case 5*	*Case 6*	*Cases 1–6*
a	8.5	5.6	14.4	12.5	13.2	14.2	13.2	13.5	13.5
b	10.0	5.1	14.4	15.4	13.5	14.6	14.6	14.4	14.5
Longitudinal deviation	1.5 (8%)	0.5 (5%)	0 (0)	2.9 (10%)	0.3 (1%)	0.4 (1%)	1.4 (5%)	0.9 (3%)	1.0 (4%)

utilized material data from characterization tests as input, providing an effective numerical-experimental mixed methodology for the analysis.

Both mechanical response and damage phenomena of the impacted nanocomposites were analyzed and a comparison between experimental and numerical results at different impact energies is reported. The main conclusions can be summarized as:

- As energy increases from 15 to 30 J, the importance of the nanoparticles distribution decreases. The variation in loading history due to nanoparticles distribution reduced from 20% to 10%, and the deviation in damage from 81 to 4%.
- The stochastic model can replicate the deviation/uncertainty of deformation and damage of the impacted panel at different local regions observed in the experiments, which is not feasible for a model with uniform material properties.
- Application of the stochastic model can help determining the range of damage tolerance under impact loading for the design of nanocomposites. The damage volume can display up to 50% variation when considering the distribution of nanoparticles.

CRediT authorship contribution statement

Dayou Ma: Conceptualization, Methodology, Software, Investigation, Validation, Visualization, Writing – original draft. **Christian Matheus dos Santos Cougo:** Resources, Investigation. **Sandro Campos Amico:** Visualization, Resources, Writing – review & editing. **Marco Giglio:** Conceptualization, Project administration, Funding acquisition.

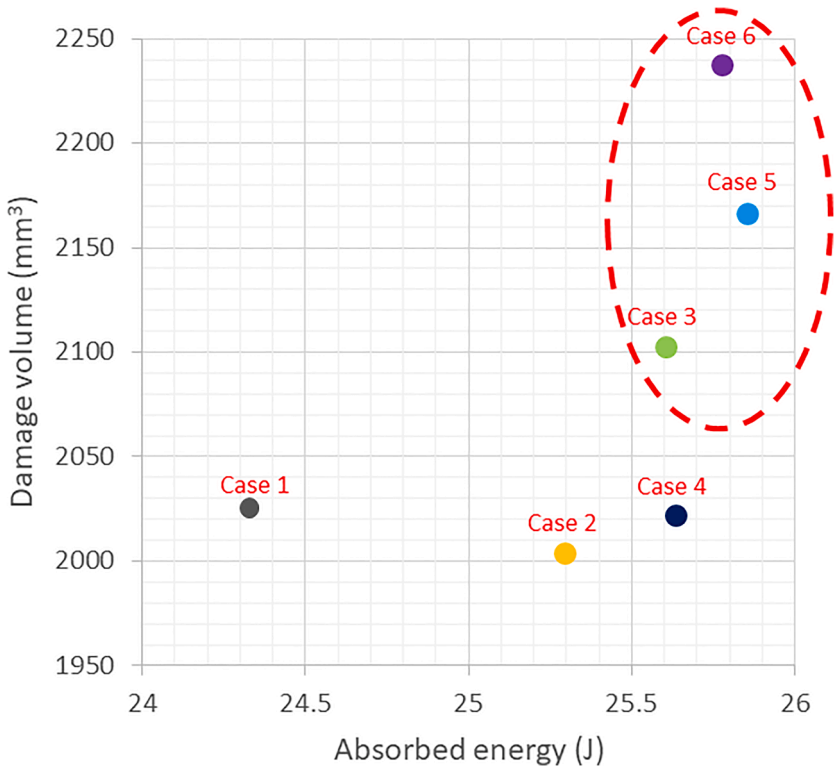

Fig. 9. Correlation between absorbed energy and damage volume for an impact energy of 30 J.

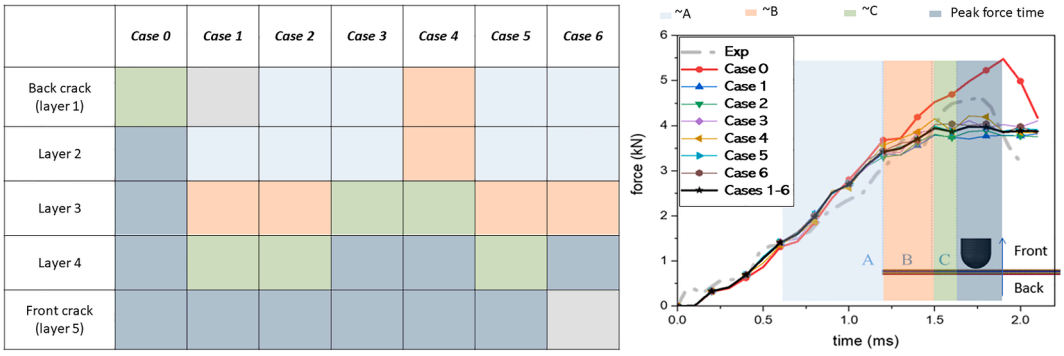

Fig. 10. Penetration history of the composite from the numerical models for an impact energy of 30 J.

Andrea Manes: Visualization, Resources, Supervision, Conceptualization, Writing – review & editing.

Declaration of Competing Interest

The authors declare that they have no known competing financial interests or personal relationships that could have appeared to influence the work reported in this paper

Data availability

Data will be made available on request.

References

[1] Mecklenburg M, Mizushima D, Ohtake N, Bauhofer W, Fiedler B, Schulte K. On the manufacturing and electrical and mechanical properties of ultra-high wt.% fraction aligned MWCNT and randomly oriented CNT epoxy composites. Carbon N Y 2015; 91:275–90. https://doi.org/10.1016/J.CARBON.2015.04.085.

[2] Liu B, Vu-Bac N, Zhuang X, Rabczuk T. Stochastic multiscale modeling of heat conductivity of Polymeric clay nanocomposites. Mech Mater 2019:103280. https://doi.org/10.1016/J.MECHMAT.2019.103280.

[3] Ma D, Giglio M, Manes A. Numerical investigation on the uniaxial compressive behavior of an epoxy resin and a nanocomposite. Eur J Mech A Solids 2022;92: 104500. https://doi.org/10.1016/j.euromechsol.2021.104500.

[4] Chiu JJ, Kim BJ, Yi GR, Bang J, Kramer EJ, Pine DJ. Distribution of nanoparticles in lamellar domains of block copolymers. Macromolecules 2007;40:3361–5. https://doi.org/10.1021/MA061503D/ASSET/IMAGES/LARGE/MA061503DF00006.JPEG.

[5] Esmaeili A, Sbarufatti C, Ma D, Manes A, Jiménez-Suárez A, Ureña A, et al. Strain and crack growth sensing capability of SWCNT reinforced epoxy in tensile and mode I fracture tests. Compos Sci Technol 2020;186:107918. https://doi.org/10.1016/j.compscitech.2019.107918.

[6] Alian AR, El-Borgi S, Meguid SA. Multiscale modeling of the effect of waviness and agglomeration of CNTs on the elastic properties of nanocomposites. Comput Mater Sci 2016;117:195–204. https://doi.org/10.1016/j.commatsci.2016.01.029.

[7] Esmaeili A, Ma D, Manes A, Oggioni T, Jiménez-Suárez A, Ureña A, et al. An experimental and numerical investigation of highly strong and tough epoxy based nanocomposite by addition of MWCNTs: tensile and mode I fracture tests. Compos Struct 2020;252:112692. https://doi.org/10.1016/j.compstruct.2020.112692.

[8] Nanni F, Mayoral BL, Madau F, Montesperelli G, McNally T. Effect of MWCNT alignment on mechanical and self-monitoring properties of extruded PET–MWCNT nanocomposites. Compos Sci Technol 2012;72:1140–6. https://doi.org/10.1016/j.compscitech.2012.03.015.

[9] Ma D, Giglio M, Manes A. An investigation into mechanical properties of the nanocomposite with aligned CNT by means of electrical conductivity. Compos Sci Technol 2020;188:107993. https://doi.org/10.1016/J.COMPSCITECH.2020.107993.
[10] Li W, Dichiara A, Bai J. Carbon nanotube–graphene nanoplatelet hybrids as high-performance multifunctional reinforcements in epoxy composites. Compos Sci Technol 2013;74:221–7. https://doi.org/10.1016/J.COMPSCITECH.2012.11.015.
[11] Yang Q, Xu C, Cheng G, Meng S, Xie W. Uncertainty quantification method for mechanical behavior of C/SiC composite and its experimental validation. Compos Struct 2019:111516. https://doi.org/10.1016/J.COMPSTRUCT.2019.111516.
[12] Balokas G, Kriegesmann B, Czichon S, Rolfes R. Stochastic modeling techniques for textile yarn distortion and waviness with 1D random fields. Compos Part A Appl Sci Manuf 2019;127:105639. https://doi.org/10.1016/j.compositesa.2019.105639.
[13] Pekmezi G, Littlefield D, Chareyre B. Statistical distributions of the elastic moduli of particle aggregates at the mesoscale. Int J Impact Eng 2019:103481. https://doi.org/10.1016/J.IJIMPENG.2019.103481.
[14] Omairey SL, Dunning PD, Sriramula S. Influence of micro-scale uncertainties on the reliability of fibre-matrix composites. Compos Struct 2018;203:204–16. https://doi.org/10.1016/j.compstruct.2018.07.026.
[15] Meguid S, Sun Y. On the tensile and shear strength of nano-reinforced composite interfaces. Mater Des 2004;25:289–96. https://doi.org/10.1016/J.MATDES.2003.10.018.
[16] Alian AR, Meguid SA. Multiscale modeling of the coupled electromechanical behavior of multifunctional nanocomposites. Compos Struct 2018;208:826–35. https://doi.org/10.1016/j.compstruct.2018.10.066.
[17] Zhao J, Song M. A computer simulation of stress transfer in carbon nanotube/polymer nanocomposites. Compos Part B Eng 2019;163:236–42. https://doi.org/10.1016/J.COMPOSITESB.2018.11.052.
[18] Alian AR, Meguid SA. Large-scale atomistic simulations of CNT-reinforced thermoplastic polymers. Compos Struct 2018;191:221–30. https://doi.org/10.1016/J.COMPSTRUCT.2018.02.056.
[19] Zhao Z, Dang H, Zhang C, Yun GJ, Li Y. A multi-scale modeling framework for impact damage simulation of triaxially braided composites. Compos Part A Appl Sci Manuf 2018;110:113–25. https://doi.org/10.1016/J.COMPOSITESA.2018.04.020.
[20] Mehdikhani M, Petrov NA, Straumit I, Melro AR, Lomov SV, Gorbatikh L. The effect of voids on matrix cracking in composite laminates as revealed by combined computations at the micro- and meso-scales. Compos Part A Appl Sci Manuf 2019;117:180–92. https://doi.org/10.1016/j.compositesa.2018.11.009.
[21] Wu Z, Zhang L, Ying Z, Ke J, Hu X. Low-velocity impact performance of hybrid 3D carbon/glass woven orthogonal composite: experiment and simulation. Compos Part B Eng 2020:108098. https://doi.org/10.1016/j.compositesb.2020.108098.
[22] Baek K, Shin H, Yoo T, Cho M. Two-step multiscale homogenization for mechanical behaviour of polymeric nanocomposites with nanoparticulate agglomerations. Compos Sci Technol 2019;179:97–105. https://doi.org/10.1016/j.compscitech.2019.05.006.
[23] Lee W, Chung I, Baek K, Im S, Cho M. Multiscale modeling to characterize electromechanical behaviors of CNT/polymer nanocomposites considering the matrix damage and interfacial debonding. Mech Adv Mater Struct 2020:1–20. https://doi.org/10.1080/15376494.2020.1861396.
[24] Ma D, Verleysen P, Chandran S, Giglio M, Manes A. A modified peridynamic method to model the fracture behaviour of nanocomposites. Eng Fract Mech 2021;247:107614. https://doi.org/10.1016/j.engfracmech.2021.107614.
[25] Nastos C, Zarouchas D. Probabilistic failure analysis of quasi-isotropic CFRP structures utilizing the stochastic finite element and the Karhunen–Loève expansion methods. Compos Part B Eng 2022;235:109742. https://doi.org/10.1016/J.COMPOSITESB.2022.109742.
[26] Ma D, González-Jiménez Á, Giglio M, dos Santos Cougo CM, Amico SC, Manes A. Multiscale modelling approach for simulating low velocity impact tests of aramid-epoxy composite with nanofillers. Eur J Mech A Solids 2021:104286. https://doi.org/10.1016/j.euromechsol.2021.104286.
[27] González-Jiménez Á, Caldeira LE, Scazzosi R, Manes A, Amico SC, Giglio M. Low velocity impact response of R-glass/epoxy composites produced by vacuum infusion. Multiscale Multidiscip Model Exp Des 2019;2:89–96. https://doi.org/10.1007/s41939-018-0029-5.
[28] Chang FK, Chang KY. A progressive damage model for laminated composites containing stress concentrations. J Compos Mater 1987;21:834–55. https://doi.org/10.1177/002199838702100904.
[29] Ma D, Manes A, Amico SC, Giglio M. Ballistic strain-rate-dependent material modelling of glass-fibre woven composite based on the prediction of a meso-heterogeneous approach. Compos Struct 2019;216:187–200. https://doi.org/10.1016/j.compstruct.2019.02.102.
[30] LS-DYNA® Keyword user's manual (R9448). Livermore Software Technology Corporation; 2018.